COMMUNICATION

Check for updates

Zr⁴⁺-terephthalate MOFs with 6-connected structures, highly efficient As(III/V) sorption and superhydrophobic properties†

Anastasia D. Pournara,[a] Sofia Rizogianni,[a] Dimitrios A. Evangelou,[a] Evangelos K. Andreou,[b] Gerasimos S. Armatas [ID][b] and Manolis J. Manos [ID]*[ac]

The use of terephthalate ligands with $C_nH_{2n+1}NH$-chains ($n \geq 6$) led to the isolation of the first examples of Zr⁴⁺-terephthalate MOFs with 6-connected frameworks. The material with hexyl-amino functional groups has been proved to be an exceptional sorbent for the removal of As(III/V) toxic species from aqueous media, whereas MOFs with heptyl to dodecyl-amino moieties are super-hydrophobic with promising oil–water separation properties.

Metal Organic Frameworks (MOFs) based on Zr⁴⁺ and multi-carboxylate ligands have attracted tremendous interest, as they combine all unique attributes of MOFs with exceptional hydrolytic stability.[1] MOFs with terephthalate ligands and derivatives of them, denoted as UiO-66 MOFs, are typical examples with 12-c nets (fcu topology), which however often present structural defects so that their overall net connectivity appears <12.[2] Our group has recently reported several Zr⁴⁺-terephthalate MOFs, bearing picolyl-2-ammonium or $CnH_{2n+1}NH$-($n \leq 4$) groups, with decreased number of linkers and 8-c frameworks.[3] The stabilization of such nets *vs.* the 12-c frameworks results from the effect of functional groups causing increased steric interactions between the ligands.[3,4] As a result of missing dicarboxylate linkers, the MOFs with the 8-c frameworks include several terminal water/hydroxy ligands.[5] The latter can be easily replaced by toxic or radioactive oxoanions and thus, these materials have been proved excellent sorbents for the removal of harmful oxoanionic species from aqueous media.[3b,6] Examples of Zr⁴⁺-terephthalate MOFs with less than 8 linkers per Zr₆ clusters remain undiscovered. The

development of synthetic strategies towards such MOFs could be of significant interest for the isolation of materials with enhanced capability towards sorption of toxic species due to the increased number of the easily replaceable terminal ligands (*e.g.* 12 terminal water/OH⁻ in 6-c nets *vs.* 8 terminal water/OH⁻ ligands in 8-c frameworks).[1d] Furthermore, such MOFs would be particularly suitable as precursor compounds for producing new materials with tuned properties through post-synthetic incorporation of functional molecules or organic linkers.[7]

Here we report the initial examples of Zr⁴⁺-terephthalate MOFs with 6-c nets, namely MOFs with the general formula $H_{22}[Zr_6O_{20}(NH_2\text{-}BDC)_x(RNH\text{-}BDC)_{3-x}]\cdot$solvent ($x \leq 0.18$, NH₂-$BDC^{2-}$ = 2-amino-terephthalate, RNH-BDC^{2-} = 2-alkyl-amino terephthalate; R = hexyl-, **HEX-MOF**; R = heptyl-, **HEPT-MOF**; R = octyl-, **OCT-MOF**; R = nonyl-, **NON-MOF**; R = dodecyl-, **DODEC-MOF**) (Fig. S1 and S2, ESI†). The new compounds are of interest not only due to their structural characteristics, but also because of the promising As(III)/(V) sorption properties of **HEX-MOF** and the oil–water separation capability of the super-hydrophobic (**HEPT-, OCT-, NON-, DODEC-MOF**) analogues.

Our initial motivation for the isolation of MOFs with long alkyl chains was the development of new hydrophobic/superhydrophobic materials. At the beginning, we targeted towards a MOF with octyl-amino functional groups, by employing solvothermal reactions in DMF-CH₃COOH at 120 °C (ESI†). Surprisingly, the BET surface areas of several samples tested were found 726–733 $m^2\ g^{-1}$, which is significantly higher from *e.g.* the reported MOF with the much shorter *n*-butyl-amino group (609 $m^2\ g^{-1}$).[3b] Then, we have decided to prepared MOFs with hexyl-, heptyl-, nonyl and dodecyl-amino groups. Again, the surface areas, especially for **HEX-MOF** (911 $m^2\ g^{-1}$) and **HEPT-MOF** (792 $m^2\ g^{-1}$), were much higher than those of known MOFs with shorter alkyl-chains (Fig. 1a, Fig. S3 and Table S1, ESI†). At the same time, TGA data were consistent with the presence of 3 rather than 4 dicarboxylate ligands per Zr₆ cluster (Fig. S4–S8 and Table S2, ESI†). These results indicated structures with 6-connected frameworks. We have thus built and optimized (*via* simulating annealing methods) models of the MOFs with 6-c nets, which were used as starting

[a] Department of Chemistry, University of Ioannina, GR-45110, Ioannina, Greece. E-mail: emanos@uoi.gr

[b] Department of Materials Science and Technology, University of Crete, GR-71003, Heraklion, Greece

[c] Institute of Materials Science and Computing, University Research Center of Ioannina, GR-45110, Ioannina, Greece
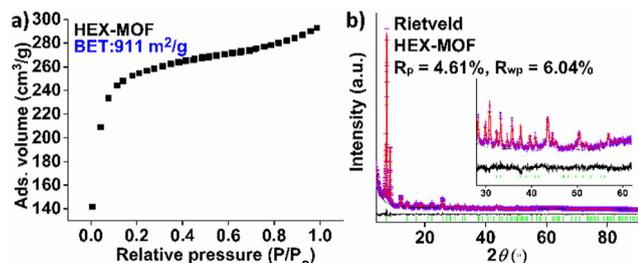
Fig. 1 (a) N_2 sorption isotherm (77 K) for **HEX-MOF**. (b) Rietveld plot of **HEX-MOF**. Violet crosses: experimental points; red line: calculated pattern; black line: difference pattern (exp-calc); and green bars: Bragg positions. Inset: Magnification of the 2θ region 30–60°.

points for Rietveld refinement (Fig. 1b and Fig. S9–S16 and refinement details in ESI†). The results of the refinements were satisfactory, which is a confirmation of the accuracy of the proposed structural models (Fig. 2 and Fig. S1, ESI†). Analysis of the structural topology of the MOFs indicate the *pcu*-net for these materials (Fig. S17, ESI†), which has been rarely observed for Zr^{4+} MOFs.[8] Importantly, the calculated (*via* poreblazer)[9] surface areas for the MOFs with 6-c nets are close to the experimental ones (Table S1, ESI†). For comparison, the theoretical BET surface area for *e.g.* a hypothetical **HEX-MOF** with 8-c net was found 502 $m^2\ g^{-1}$ (*i.e.* much smaller than the experimental value of 911 $m^2\ g^{-1}$) (Fig. 1a). Despite the low net connectivity, **HEX-MOF** remains highly crystalline after treatment with either strongly acidic (pH ∼ 0) or alkaline (pH ∼ 12) solution for 12 h, as shown by PXRD data and Le Bail analysis (Fig. S18, ESI†). Furthermore, the crystallinity of **HEX-MOF** is largely retained after treatment of the MOF at 150 and 200 °C under vacuum (Fig. S19 and S20, ESI†).

We should also note that ^1H NMR data for the MOFs digested in $NaOH/D_2O$ revealed that the linkers largely preserve their integrity in the MOFs' structures, since the decomposition of alkyl-amino-terephthalate to (non-alkylated) amino-terephthalate ligands was found ≤6% (ESI† and Fig. S21). Additional characterization data (IR, SEM) for the MOFs are provided in ESI† (Fig. S22–S27). We should also mention that the TGA and BET surface area data for the MOF with pentyl-amino functional groups were inconsistent from sample to sample, whereas MOFs with decyl- and undecyl-amino BDC^{2-}
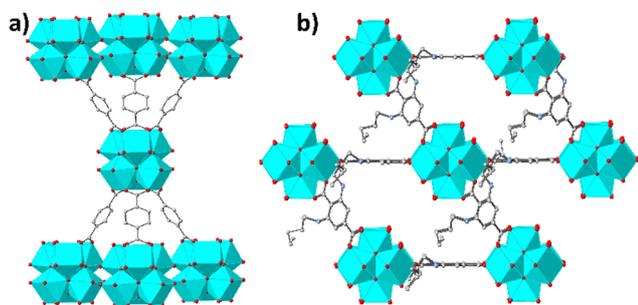

Fig. 2 Representation of (a) the cluster connectivity and (b) framework structure of **HEX-MOF** (C, gray; O, red; N, blue; and Zr turquoise), as obtained *via* the Rietveld refinement. The H atoms and the solvent molecules in the structural representation of **HEX-MOF** were omitted for clarity.

linkers showed limited crystallinity. Thus, the above MOFs were not studied in detail.

The reason for the stabilization of 6-c nets for the **HEX-**, **HEPT-**, **OCT-** and **DODEC-MOFs** is clearly related to the steric interactions between the side alkyl-amino groups that permit the accumulation of limited $C_nH_{2n+1}NH\text{-}BDC^{2-}$ linkers around the Zr_6 clusters. From the previous publication of our group,[3b] it turns out that the steric interactions between side groups with ethyl to butyl moieties allow the incorporation of 4 linkers per Zr_6 unit. However, based on the experimental data presented here, these interactions appear to be significantly stronger for ligands with longer alkyl-amino chains, thus leading to the stabilization of 6-c nets.

HEX-MOF shows a highly porous structure and multiple labile (terminal) water/hydroxy ligands. The latter are known to be easily replaced by anions or neutral molecules.[7a] Thus, we investigated the capability of **HEX-MOF** to sorb As(III/V) species, which are well known for their toxic effects, in detail. As(III/V) variable-time sorption studies revealed that both toxic species are removed from aqueous solutions within a few minutes. Kinetic data obeyed to the pseudo-second order model (Fig. S28 and Table S3, ESI†). Such a kinetic model indicates strong interactions between sorbed species and MOF sorbent. Importantly, after the 2nd min of contact, the As content was calculated to be lower than the upper limit of 10 ppb which has been established by WHO and US-EPA for As in drinking water (Fig. 3a). The As(v) sorption isotherm data of **HEX-MOF** can be fitted very well with the Langmuir model showing maximum sorption capacity as high as 104 ± 8 mg As g^{-1} of sorbent (Fig. 3c and Table S4, ESI†), close to the calculated value (116 mg g^{-1}) for the incorporation of 3 As per formula unit. In contrary, the As(III) sorption isotherm consists of two components, which can be attributed to a combination of surface binding and pore filling processes.[1f] The total As sorption capacity was calculated to be 198 ± 5 mg As g^{-1} (Fig. 3b and Table S4, ESI†), whereas the sorption capacity (98 mg As g^{-1}) observed in the second step is in good agreement with the calculated value for the insertion of 3 As species per Zr_6 cluster. The As(III/V)-loaded sorbent can be easily regenerated by treatment with acidic solution, followed by washing with a basic MeOH solution. The regenerated sorbent fully retained the As(III/V) sorption efficiency and the crystallinity of the pristine material even after 4 cycles of sorption (Fig. S29 and S30, ESI†). Further sorption studies, conducted on As-containing samples of a wide pH range from pH ∼ 1 to pH ∼ 12, revealed that **HEX-MOF** retains its efficiency to remove As(III/V) even under highly acidic or alkaline conditions with sorption percentages higher than 96% (Fig. S31, ESI†). Furthermore, the sorption capacity of **HEX-MOF** toward As species is exceptional (removal percentages > 95%) even in the presence of 1000-fold excess of several anions, including the highly competitive HPO_4^{2-} species (Fig. S32, ESI†). In addition, **HEX-MOF** showed excellent performance (removal percentages 98.8–99.8%) for the removal of As(III) and As(v) from genuine water samples (Fig. S32, ESI†) containing a mixture of cations and anions in relatively high concentrations (Table S5, ESI†).
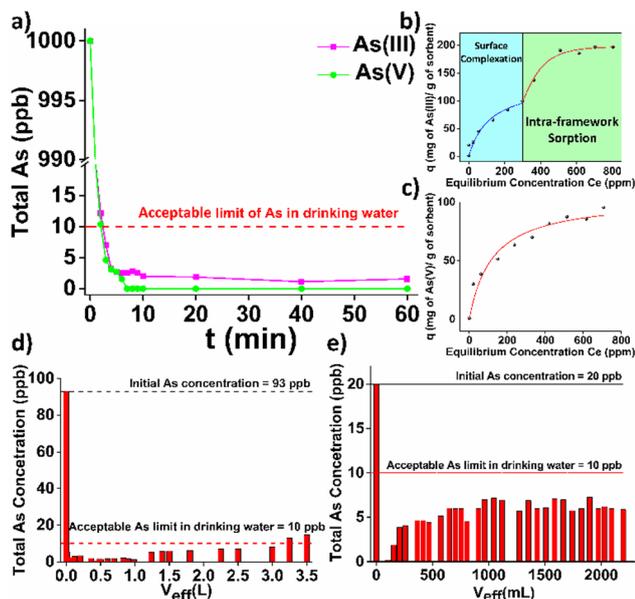
Fig. 3 (a) Kinetic study of **HEX-MOF** towards As(III) (purple line) and As(V) (green line). (Initial As concentration = 1000 ppb), (b) As(III) and (c) As(V) sorption isotherms for **HEX-MOF** at pH = 7. The solid lines represent the fitting of the data with the isotherms models (ESI†). (d) As(V) sorption under continuous flow conditions for **HEX-MOF@cotton fabric** (initial As concentration = 93 ppb in artificially contaminated bottled water). (e) As(III) sorption under continuous flow conditions for **HEX-MOF**/calcium alginate beads (initial As concentration = 20 ppb in artificially contaminated bottled water). The As content, in all above data, represents the total As amount and not that of oxo-arsenic species.
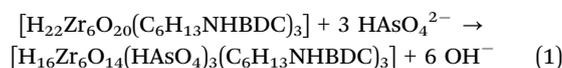
Aiming in practical applications, we have also immobilized **HEX-MOF** in cotton fabric, which was pre-coated with polydopamine (PDA). PDA includes several catecholic units, which can form strong bonds with Zr^{4+} centers. Thus, PDA-coated substrates are ideal for immobilizing Zr^{4+} MOFs.[2e] Indeed, we have been able to fabricate cotton materials loaded with **HEX-MOF** by applying an *in situ* coating method (Fig. S33, ESI†). **HEX-MOF@cotton fabric** was utilized for treatment of natural spring water intentionally contaminated with As(V) (93 ppb) under continuous flow conditions and was found capable of decontaminating more than 3 L of the polluted water sample (Fig. 3d and Fig. S34, ESI†).

As an alternative approach to use **HEX-MOF** for removal of toxic species under flow, we have prepared **HEX-MOF**/calcium alginate beads which have been used as a stationary phase in sorption columns for removal of As(III) from artificially contaminated bottled water solution (Fig. S34 and S35, ESI†). Similarly to the immobilized fabric sorbent, **HEX-MOF** in the form of beads achieved to reduce the amount of As in the effluent under the acceptable limit in drinking water, even after 2 L have been passed through the column (Fig. 3e).

A detailed comparison of **HEX-MOF** with other state-of-the art sorbents (Tables S6 and S7, ESI†) revealed that **HEX-MOF** is among the best As(III/V) sorbents in terms of sorption kinetics, combining also appreciable As(III/V) maximum sorption capacities. Importantly, the As(III/V) sorption of **HEX-MOF** is retained exceptional even in the presence of tremendous excess (up to 1000-fold)
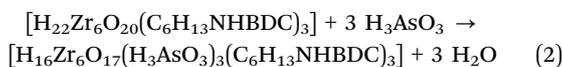
of competitive species and in a wide pH range (1–12), with such performance not shown by the reported sorbents. Not least, **HEX-MOF** is a rare case of a MOF with demonstrated efficiency for capture of As(III/V) under realistic conditions and continuous flow.

The zeta potential of **HEX-MOF** was found close to 0 (0.148 mV). Thus, it is unlikely that **HEX-MOF** will interact with As(V) oxoanions *via* electrostatic interactions. Furthermore, ^{1}H NMR data on filtrates after sorption studies in D_2O (ESI†) revealed no release of organic species and thus, the sorption process does not proceed *via* exchange of organic ligands by As(V) oxoanions (Fig. S36, ESI†). Considering that (a) **HEX-MOF** absorbs 3 moles of As(V) per formula unit, (b) As(V) exists as a mixture of $H_2AsO_4^-$ and $HAsO_4^{2-}$ at pH = 7,[10] and (c) the hard Zr^{4+} will prefer coordination with the divalent $HAsO_4^{2-}$ rather than the monoanionic $H_2AsO_4^-$, the As(V) sorption process may be described with the following equation:

$$[H_{22}Zr_6O_{20}(C_6H_{13}NHBDC)_3] + 3\ HAsO_4^{2-} \rightarrow$$
$$[H_{16}Zr_6O_{14}(HAsO_4)_3(C_6H_{13}NHBDC)_3] + 6\ OH^- \quad (1)$$

Thus, 3 $HAsO_4^{2-}$ anions replace 6 terminal hydroxyl ligands and each of the As(V) oxoanions is expected to be inserted as bridging ligand to the Zr_6 cluster unit (Fig. 4a). Rietveld refinement confirmed the accuracy of the structure with 3 $HAsO_4^{2-}$ bridging ligands per Zr_6 cluster (Fig. S37, ESI†). Finally, the high preference of **HEX-MOF** towards As(V) anions, as demonstrated *via* sorption experiments in the presence of multiple ions in large excess, is attributed to the excellent ligation capability of As(V) species for Zr^{4+} ions.[2e]

In addition, taking into account that (a) As(III) is present as the neutral H_3AsO_3 form at pH = 7,[10] and (b) 3 As(III) species (per formula unit) are inserted inside the framework of **HEX-MOF**, the intra-framework As(III) sorption process can be described *via* the following equation:

$$[H_{22}Zr_6O_{20}(C_6H_{13}NHBDC)_3] + 3\ H_3AsO_3 \rightarrow$$
$$[H_{16}Zr_6O_{17}(H_3AsO_3)_3(C_6H_{13}NHBDC)_3] + 3\ H_2O \quad (2)$$

Therefore, 3 H_3AsO_3 exchange 3 terminal H_2O ligands and each of the inserted As(III) species may be coordinated as monodentate ligand to the Zr^{4+} ions of the cluster unit (Fig. 4b). Again, Rietveld refinement verified the reliability of the proposed structural model (Fig. S37, ESI†). Further verification of the facile
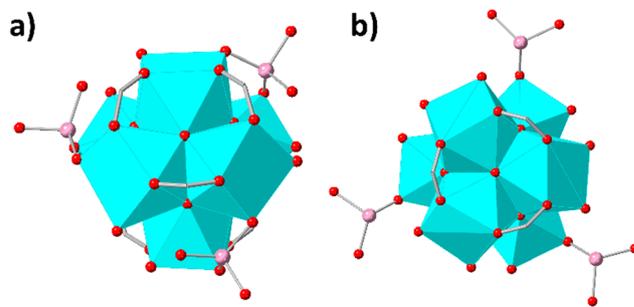

Fig. 4 The coordination mode of (a) As(V) and (b) As(III) species (Arsenic atoms shown as pink balls) in the structures of **HEX-MOF/As(V)** and **HEX-MOF/As(III)** respectively, as determined *via* Rietveld refinement.
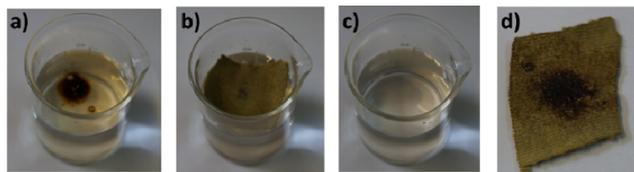
Fig. 5 (a) Crude oil in water sample, (b) sorption of crude oil on **HEX-MOF@cotton fabric**, (c) oil-free water (obtained after the treatment with the fabric sorbent), (d) **HEX-MOF@cotton fabric** after crude oil sorption.

exchange of water by As(III) species was provided *via* theoretical calculations revealing higher charge of O atoms in H_3AsO_3 *vs.* that of O in H_2O (Fig. S38, ESI†) and thus, a more powerful ligation capability of As(III) towards the hard Zr^{4+} ions.

In addition, XPS data confirmed the oxidation states (III) and (v) for the As species in As(III) and As(v)-loaded materials respectively (Fig. S39, ESI†). Further characterization of the As(v) and As(III)-loaded materials has been performed *via* IR, BET surface area measurements and EDS analysis (Fig. S40–S42, ESI†).

The MOFs described here are based on linkers with long alkyl chains and thus, are expected to display hydrophobic or superhydrophobic properties.[11] Indeed, the water contact angles for the **HEPT-**, **OCT-**, **NON-** and **DODEC-MOFs** were determined 150–154 deg implying superhydrophobicity (Fig. S43 and S44, ESI†). In contrast, **HEX-MOF** is readily wettable by water (contact angles < 10 deg). In addition, the superhydrophobic MOFs, *e.g.* **DODEC-MOF**, are easily dispersed in non-polar solvents and are not miscible with water, in contrast to the hydrophilic **HEX-MOF** forming suspension in aqueous media (Fig. S45, ESI†). We should also mention that **HEPT-**, **OCT-**, **NON-** and **DODEC-MOFs** retain their superhydrophobic properties in different types of aqueous media (distilled water, lake water, seawater) and in a wide pH range (Fig. S43, ESI†).

Although several hydrophobic/superhydrophobic MOFs have been developed in powder form,[11a] less efforts have been devoted to the incorporation of such materials into stable substrates, that would be easily recovered after use in *e.g.* oil/water separation processes.[11b] Thus, **HEPT-**, **OCT-**, **NON-** and **DODEC-MOFs** were immobilized in cotton fabrics, with the same method applied for **HEX-MOF** (see above). The modified fabrics are superhydrophobic with water contact angles of 151–156 deg (Fig. S46 and S47, ESI†). We have then investigated the capability of **DODEC-MOF@fabric** for removal of crude oil from water under both static and continuous flow conditions. As can be seen in Fig. 5 (Fig. S48 and Video in ESI†), **DODEC-MOF@fabric** could eliminate rapidly crude oil from the water in either static or continuous flow mode, thus revealing its potential for application in oil spill cleanup and as an oil filter.

In summary, the utilization of terephthalate ligands with long alkyl-amino chains leads to the stabilization of Zr^{4+} MOFs with unusual 6-c nets. The resulted materials show interesting and diverse properties ranging from sorption of toxic species to oil–water separation capability. The above synthetic approach creates opportunities for the isolation of a series of Zr^{4+} MOFs

with low net-connectivity and multiple terminal water/hydroxyl ligands, by utilizing a variety of multi-carboxylate ligands with elongated substituent groups. Such research efforts are underway in our laboratory.

Conflicts of interest

There are no conflicts to declare.

Notes and references

1 (*a*) L. Feng, J. Pang, P. She, J. L. Li, J. S. Qin, D. Y. Du and H. C. Zhou, *Adv. Mater.*, 2020, **32**, 2004414; (*b*) D. Feng, Z. Y. Gu, J. R. Li, H. L. Jiang, Z. Wei and H. C. Zhou, *Angew. Chem., Int. Ed.*, 2012, **51**, 10307–10310; (*c*) V. Bon, I. Senkovska, I. A. Baburin and S. Kaskel, *Cryst. Growth Des.*, 2013, **13**, 1231–1237; (*d*) Y. Bai, Y. Dou, L.-H. Xie, W. Rutledge, J.-R. Li and H.-C. Zhou, *Chem. Soc. Rev.*, 2016, **45**, 2327–2367; (*e*) H. Wang, X. Dong, J. Lin, S. J. Teat, S. Jensen, J. Cure, E. V. Alexandrov, Q. Xia, K. Tan, Q. Wang, D. H. Olson, D. M. Proserpio, Y. J. Chabal, T. Thonhauser, J. Sun, Y. Han and J. Li, *Nat. Commun.*, 2018, **9**, 1745; (*f*) Y. Georgiou, S. Rapti, A. Mavrogiorgou, G. Armatas, M. J. Manos, M. Louloudi and Y. Deligiannakis, *Sci. Rep.*, 2020, **10**, 9358.
2 (*a*) M. Perfecto-Irigaray, G. Beobide, O. Castillo, I. Da Silva, D. García-Lojo, A. Luque, A. Mendia and S. Pérez-Yáñez, *Chem. Commun.*, 2019, **55**, 5954–5957; (*b*) J. Ren, M. Ledwaba, N. M. Musyoka, H. W. Langmi, M. Mathe, S. Liao and W. Pang, *Coord. Chem. Rev.*, 2017, **349**, 169–197; (*c*) G. C. Shearer, S. Chavan, S. Bordiga, S. Svelle, U. Olsbye and K. P. Lillerud, *Chem. Mater.*, 2016, **28**, 3749–3761; (*d*) D. Feng, W. C. Chung, Z. Wei, Z. Y. Gu, H. L. Jiang, Y. P. Chen, D. J. Darensbourg and H. C. Zhou, *J. Am. Chem. Soc.*, 2013, **135**, 17105–17110; (*e*) A. D. Pournara, E. Moisiadis, V. Gouma, M. J. Manos and D. L. Giokas, *J. Environ. Chem. Eng.*, 2022, **10**, 107705.
3 (*a*) S. A. Diamantis, A. D. Pournara, E. D. Koutsouroubi, C. Moularas, Y. Deligiannakis, G. S. Armatas, A. G. Hatzidimitriou, M. J. Manos and T. Lazarides, *Inorg. Chem.*, 2022, **61**, 7847–7858; (*b*) A. D. Pournara, S. Rapti, A. Valmas, I. Margiolaki, E. Andreou, G. S. Armatas, A. C. Tsipis, J. C. Plakatouras, D. L. Giokas and M. J. Manos, *J. Mater. Chem. A*, 2021, **9**, 3379–3387.
4 Z. Chen, S. L. Hanna, L. R. Redfern, D. Alezi, T. Islamoglu and O. K. Farha, *Coord. Chem. Rev.*, 2019, **386**, 32–49.
5 S. Yuan, W. Lu, Y. P. Chen, Q. Zhang, T. F. Liu, D. Feng, X. Wang, J. Qin and H. C. Zhou, *J. Am. Chem. Soc.*, 2015, **137**, 3177–3180.
6 (*a*) W. Xiang, Y. Zhang, Y. Chen, C. J. Liu and X. Tu, *J. Mater. Chem. A*, 2020, **8**, 21526–21546; (*b*) F. Ahmadijokani, H. Molavi, M. Rezakazemi, S. Tajahmadi, A. Bahi, F. Ko, T. M. Aminabhavi, J. R. Li and M. Arjmand, *Prog. Mater. Sci.*, 2022, **125**, 100904.
7 (*a*) L. Feng, G. S. Day, K. Y. Wang, S. Yuan and H. C. Zhou, *Chemistry*, 2020, **6**, 2902–2923; (*b*) H. Lyu, O. I. F. Chen, N. Hanikel, M. I. Hossain, R. W. Flaig, X. Pei, A. Amin, M. D. Doherty, R. K. Impastato, T. G. Glover, D. R. Moore and O. M. Yaghi, *J. Am. Chem. Soc.*, 2022, **144**, 2387–2396.
8 L. H. Xie, X. M. Liu, T. He and J. R. Li, *Chemistry*, 2018, **4**, 1911–1927.
9 L. Sarkisov and A. Harrison, *Mol. Simul.*, 2011, **37**, 1248–1257.
10 P. L. Smedley and D. G. Kinniburgh, *Appl. Geochem.*, 2002, **17**, 517–568.
11 (*a*) S. Mukherjee, S. Sharma and S. K. Ghosh, *APL Mater.*, 2019, **7**, 050701; (*b*) D. Kim, D. W. Kim, O. Buyukcakir, M.-K. Kim, K. Polychronopoulou and A. Coskun, *Adv. Funct. Mater.*, 2017, **27**, 1700706.